A Journal of the Gesellschaft Deutscher Chemiker

Angewandte International Edition GDCh Chemie

www.angewandte.org

Accepted Article

Title: Biomimetic synthesis of rhytidenone A and elucidation of mode of action of the cytotoxic rhytidenone F

Authors: Xiaoguang Lei, Zongwei Yue, Hiuchun Lam, Kaiqi Chen, Ittipon Siridechakorn, Yaxi Liu, and Khanitha Pudhom

To be cited as: *Angew. Chem. Int. Ed.* 10.1002/anie.201914257
Angew. Chem. 10.1002/ange.201914257

Link to VoR: http://dx.doi.org/10.1002/anie.201914257
http://dx.doi.org/10.1002/ange.201914257

WILEY-VCH

10.1002/anie.201914257

WILEY-VCH

RESEARCH ARTICLE

Biomimetic synthesis of rhytidenone A and elucidation of mode of action of the cytotoxic rhytidenone F

Zongwei Yue,[a,b,+] Hiu C. Lam,[b,+] Kaiqi Chen,[b] Ittipon Siridechakorn,[b] Yaxi Liu,[b] Khanitha Pudhom,[c] Xiaoguang Lei [b]*

Abstract: Rhytidenones family are spirobisnaphthalene natural products isolated from mangrove endophytic fungus *Rhytidhysteron rufulum* AS21B. The biomimetic synthesis of complex rhytidenone A was achieved via a sequence of Michael reaction, aldol and lactonization cascade in a single step, from the proposed biosynthetic precursor rhytidenone F. Moreover, the mode of action of the highly cytotoxic rhytidenone F has been investigated. The pulldown assay coupled with mass spectrometry analysis revealed the target protein PA28γ is covalently attached to rhytidenone F at the Cys92 residue. The interactions of rhytidenone F with PA28γ would lead to the accumulation of p53 which is an essential tumor suppressor in humans. Consequently, the Fas-dependent signalling pathway will be activated to initiate cellular apoptosis. Our studies have identified the first small molecule inhibitor targeting PA28γ, suggesting rhytidenone F may serve as a promising natural product lead for future anticancer drug development.

Introduction

p53 is an essential tumor suppressor in humans.[1] Loss or mutation of p53 is strongly associated with various cancers.[2] Extensive studies to develop drugs that could activate or restore the p53 pathway have now reached clinical trials.[3] Fundamentally, discovery of small molecules targeting p53 pathway with new mode of action may further stimulate many exciting new approaches to cancer drug discovery. Spirobisnaphthalenes consist of two naphthalene-derived C10 units joining together through a spiroketal linkage, belong to a novel family of natural products isolated from fungi.[4-5] They possess a variety of biological properties,[6] including antimicrobial,[7-8] antiplasmodial,[9] antileishmanial,[10] nematicidal,[11] and antitumor activities.[12] In 2014, Pudhom and coworkers identified a family of novel spirobisnaphthalene compounds from endophytic fungi *Rhytidhysteron rufulum* AS21B, namely rhytidenones A-F (Scheme 1).[13] Rhytidenone F (**2**) shows excellent cytotoxic activity against Ramos (Burkitt's lymphoma) and H1975 (non-small cell lung cancer) cells,[14] but the mode of action remains elusive. Moreover, rhytidenone A (**6**) bears the most complex structure in the rhytidenone family containing 6 contiguous stereocenters and a spirocycle, which could be biogenetically derived from rhytidenone F (**2**).

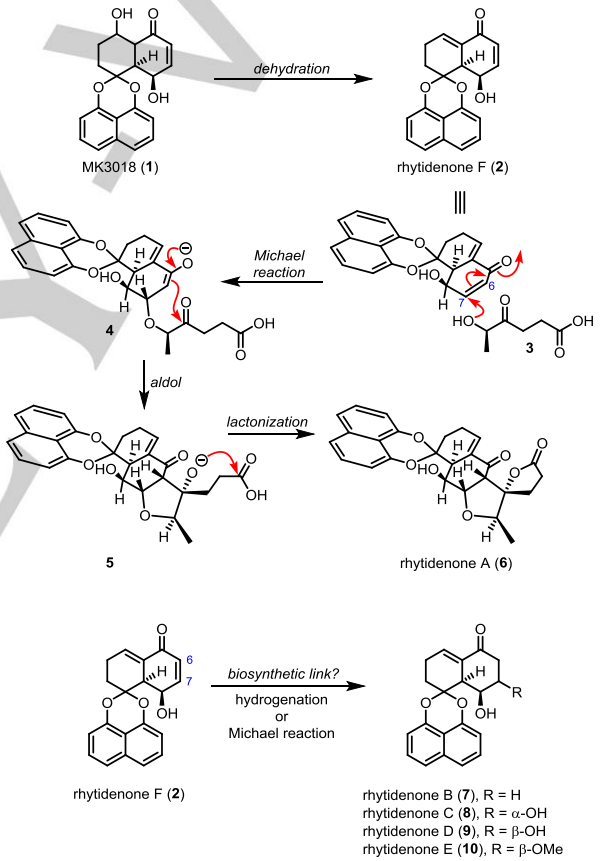

Scheme 1. Proposed biosynthetic connections of rhytidenones A-F and MK3018 from *Rhytidhysteron rufulum* AS21B.[13, 15]

We postulate the biosynthesis of rhytidenones natural products could be derived from MK3018 (**1**), a natural product which is co-isolated from *Rhytidhysteron rufulum* AS21B (Scheme 1).[15-16] Dehydration of MK3018 (**1**) would afford rhytidenone F (**2**). Union of rhytidenone F (**2**) with hydroxyketone **3** via a series of cascade reaction could give rhytidenone A (**6**). Hydroxyketone **3** is a secondary metabolite which is derived from *α*-ketoglutarate and acetaldehyde, common intermediates from citric acid cycle and ethanol metabolism respectively.[17-19] Our proposed biosynthesis of rhytidenone A (**6**) first involves a Michael reaction of the

[a] Z. Yue[+]
School of Life Sciences, Peking University, Beijing 100871, People's Republic of China
[b] Z. Yue[+], Dr. H. C. Lam[+], K. Chen, Dr. I. Siridechakorn, Y. Liu, Prof. Dr. X. Lei
Beijing National Laboratory for Molecular Sciences, State Key Laboratory of Natural and Biomimetic Drugs, Key Laboratory of Bioorganic Chemistry and Molecular Engineering of Ministry of Education, Department of Chemical Biology, College of Chemistry and Molecular Engineering, Synthetic and Functional Biomolecules Center, and Peking-Tsinghua Center for Life Sciences, Peking University, Beijing 100871, People's Republic of China
Email: xglei@pku.edu.cn
[c] Prof. Dr. K. Pudhom
Department of Chemistry, Faculty of Science, Chulalongkorn University, Bangkok 10330 Thailand
[+] These authors contributed equally to this work

Supporting information for this article is given via a link at the end of the document.

10.1002/anie.201914257

secondary alcohol **3** to the unsaturated ketone of rhytidenone F (**2**). The resulting enolate **4** would then attack the ketone to give alkoxide **5**, followed by lactonization to afford rhytidenone A (**6**) (Scheme 1). Similarly, selective hydrogenation of $\Delta^{6,7}$-alkene of rhytidenone F (**2**) could give rhytidenone B (**7**), while Michael reaction by water or methanol could deliver rhytidenones C-E (**8** – **10**) respectively.

Results and Discussion

Herein, we report a biomimetic synthesis of rhytidenone A (**6**). First, hydroxyketone **14** can be obtained from **12** which can be accessed from a 3-step transformation of acetylfuran **11**.[20-21] Hydrogenation of **12** by Zn and AcOH afforded **13**,[22] followed by ring opening of lactone by NaOH and MeOH to give **14** (Scheme 2A). In this study, rhytidenone F (**2**) was obtained either from isolation of *Rhytidhysteron rufulum* AS21B or dehydration of the more naturally abundant MK3018 (**1**).[14] After screening a few conditions, we found heating **1** with $PhB(OH)_2$[23] and acetic acid in reflux PhMe afforded rhytidenone F (**2**), which matches the spectroscopic data from the isolated **2**.

With rhytidenone F (**2**) and **14** in hand, we began our investigation on the biomimetic cascade transformation towards rhytidenone A (**6**). After screening both acidic and basic conditions (Scheme 2D), we have discovered stirring **2** and **14** in *p*TSA·H_2O in $PhCF_3$ at room temperature gave rhytidenone A (**6**) in 39% yield along with diastereoisomer **15** (Scheme 2B). **15** is presumably derived from the non-stereoselective aldol reaction where enolate **4** could attack either side of the ketone. Our DFT calculation suggested rhytidenone A (**6**) is thermodynamically more stable than *epi*-9-rhytidneone A **15** by 2.85 kcal mol^{-1} which is consistent to our experimental results (Scheme 2C). To our surprise, the optical rotation of rhytidenone A (**6**) is opposite to the reported value from the isolation. Our single crystal X-ray crystallography has unambiguously confirmed the absolute configuration of rhytidenone A (**6**). Unfortunately, we were unable to obtain natural rhytidenone A (**6**) for comparison despite multiple isolation attempts from *Rhytidhysteron rufulum* AS21B. After discussion with the authors of the original natural product isolation paper, we

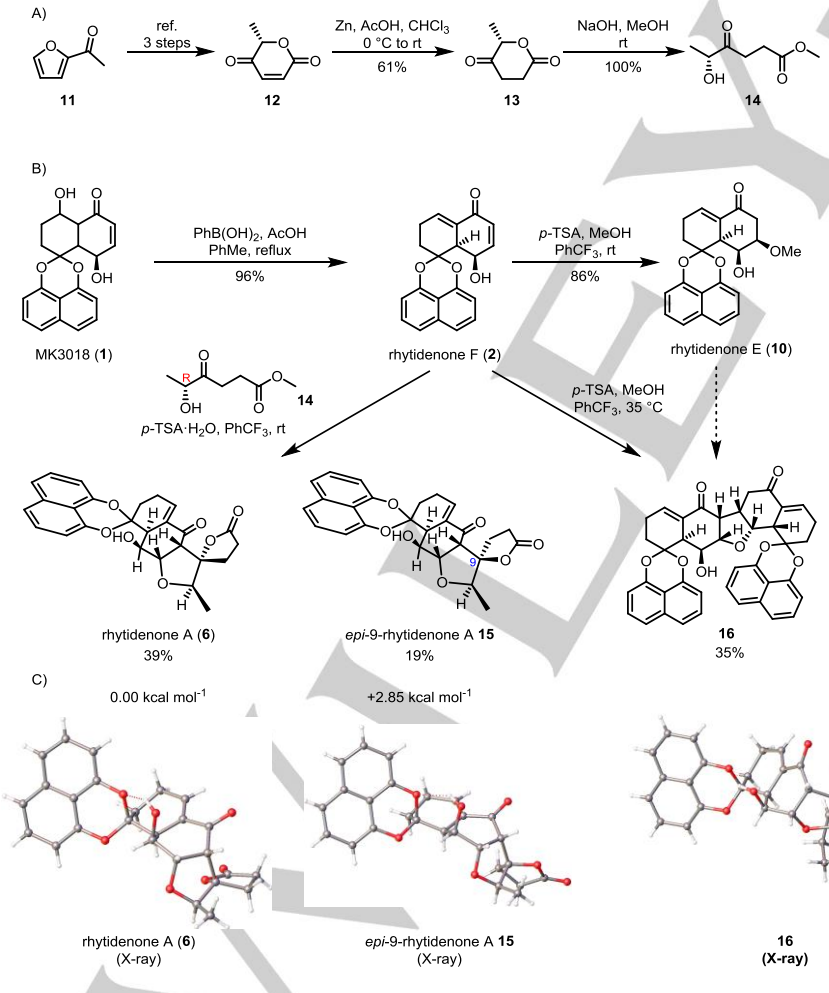

D)

Reagents	Conditions	Results
CSA	CH_2Cl_2, reflux	no reaction
TFA	CH_2Cl_2, reflux	no reaction
K_2CO_3	$CHCl_3$, reflux	no reaction
$BF_3{\cdot}OEt_2$	PhMe, rt	not desired product
p-TSA·H_2O	PhMe, rt	rhytidneone A, 3%
PPTS	PhMe, rt	no reaction
PPTS, NH_3	PhMe, rt	no reaction
p-TSA·H_2O, NH_3	PhMe, rt	no reaction
p-TSA·H_2O, NH_4OH	PhMe, rt	no reaction
p-TSA·H_2O	$PhCF_3$, rt	rhytidenone A, 39%
p-TSA·H_2O	$PhCF_3$, 0 ºC to rt	rhytidenone A, 20%
p-TSA·H_2O	$PhCF_3$, 40 ºC	rhytidenone A, 20%
p-TSA·H_2O	PhCl, rt	not desired product
p-TSA·H_2O	PhBr, rt	not desired product

Scheme 2. A) Synthesis of the methyl ester **14**; B) Biomimetic synthesis of rhytidenone A (**6**) and rhytidenone E (**10**); C) Relative Gibbs free energies of **6** and **15** calculated at DFT/m06-2x-6-311G(d,p) level of theory; D) Selected screened conditions for the biomimetic cascade reaction.

10.1002/anie.201914257

believe that the previous optical rotation was wrongly measured due to the small amount of natural product sample.

Next, subjecting rhytidenone F (**2**) in *p*TSA in the presence of MeOH gave rise to rhytidenone E (**10**) in 86% yield. Interestingly, only a single diastereoisomer was observed in the reaction suggesting the Michael reaction with methanol is stereoselective. The spectroscopic data of rhytidenone E (**10**) matches the reported literature data.[13] Furthermore, we have observed an interesting dimerization product **16** when rhytidenone E (**10**) was heated at 35 °C during evaporation of solvent in the presence of acid (Scheme 2B), presumably via a double Michael reactions. The structure of dimer **16** was confirmed by single crystal X-ray crystallography. The biomimetic synthesis of rhytidenone A (**6**) from rhytidenone F (**2**) has provided insights towards the biosynthesis of the rhytidenones family. Although the biomimetic transformation of rhytidenone F (**2**) to rhytidenone A (**6**) is not fully diastereoselective in the aldol step, considering both **2** and **3** are natural products and the reaction took place in relative mild conditions, we speculate **15** might be an "undiscovered natural product".

Table 1A. IC_{50} of compounds against HeLa cells.

Compound	IC_{50} (μM)
MK3018 (1)	0.97 (±0.08)
rhytidenone F (2)	0.21 (±0.10)
rhytidenone E (10)	1.38 (±0.01)
dimer 16	19.8 (±3.90)
rhytidenone A (6)	9.35 (±1.91)
***epi*-9-rhytidenone A (15)**	1.51 (±0.19)

Table 1B. The anti-proliferation effects of rhytidenone F (**2**) against different cancer cell lines.

Cell line	IC_{50} (μM)
HEK293T (non-pathological cell)	0.51 (±0.23)
K562 (leukemia)	0.30 (±0.06)
HL-60 (leukemia)	0.05 (±0.03)
NB4 (leukemia)	0.07 (±0.02)
Ramos (lymphoma)	0.01 (±0.01)
Hut-78 (lymphoma)	0.13 (±0.01)
HCT-116 (colon cancer)	0.07 (±0.06)
HeLa (cervical cancer)	0.21 (±0.10)
HEPG2 (liver cancer)	0.44 (±0.18)
KB (oral cancer)	0.20 (±0.05)
A549 (lung cancer)	0.39 (±0.17)
MCF-7 (breast cancer)	0.81 (±0.32)
MDA-MB-231 (breast cancer)	0.41 (±0.13)
SK-MEL-28 (melanoma)	0.82 (±0.36)

After total synthesis, we then investigated the preliminary cytotoxicity of the natural products and two derivatives towards HeLa cells, where rhytidenone F (**2**) is the most potent one (Table 1A). We observed **2** can trigger cancer cells death in low dose through inducing cell apoptosis. We have further investigated the anticancer efficacy of rhytidenone F (**2**) to 13 different human tumor cell lines representing 9 different cancer types. (Table 1B) The tumor cells were treated with increasing concentration of rhytidenone F (**2**) for 24 h or 72 h. Subsequently, cell viability was assessed using the cell-titer Glo kit. Rhytidenone F (**2**) shows potent anticancer activity against the tumor cell lines with IC_{50} values of 0.01 ~ 0.82 μM (Table 1B). In addition, rhytidenone F (**2**) is more toxic towards leukemia and lymphoma cell lines than solid tumors. These results suggest rhytidenone F (**2**) might be a promising agent for anticancer drug development.

Cell death occurs in four major manners: apoptosis (type I cell death), autophagic cell death (type II), necrosis (type III) and ferroptosis.[24-25] Apoptosis, a programmed cell death, is regarded as a caspase-dependent process, characterized by cell shrinkage and DNA fragmentation.[26] To determine if rhytidenone F (**2**) induces apoptosis or other types of cell death, we treated HeLa cells with rhytidenone F (**2**) for 24 h, and subsequently observed the effects of morphological features. Upon the treatment of rhytidenone F (**2**), HeLa cells appeared shrinkage and lost the capacity of adherence (Figure S1a). Moreover, the activation of caspase 3 and poly ADP-ribose polymerase (PARP) proteolysis were clearly noticeable in western blot when exposed to rhytidenone F (**2**) (Figure S1b), suggesting rhytidenone F (**2**) triggers caspase-dependent cell apoptosis. Additionally, rhytidenone F (**2**) can induce genomic DNA fragmentation which is another hallmark of apoptosis (Figure S1c.). We also observed that rhytidenone F (**2**) has no significant effect on cell cycle comparing to the control group by by flow cytometry analysis (Figure S1d).

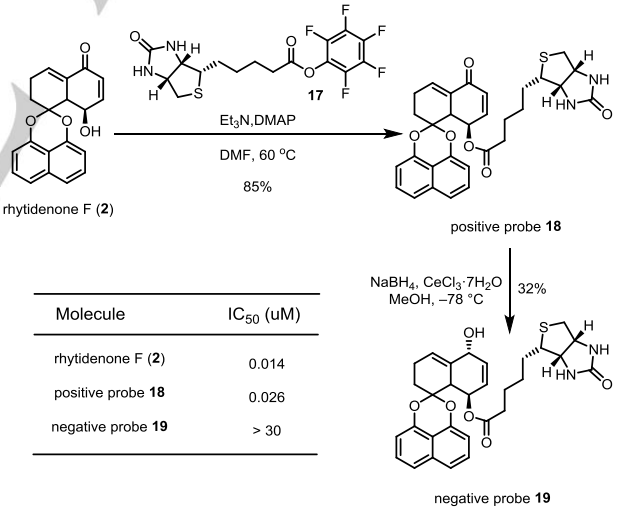

Scheme 3. Syntheses and biological evaluation of both positive and negative rhytidenone F probes for target identification. Biological activity was evaluated against Ramos cells.

Our next objective is to identify the cellular target proteins that directly interacts with rhytidenone F (**2**) in order to further elucidate its mode of action. Since the electrophilic unsaturated ketones moieties of rhytidenone F (**2**) could be good Michael acceptors to form covalent bonds with nucleophilic residues of proteins (e.g. cysteines) to give rise to the biological activity,[27] we

10.1002/anie.201914257

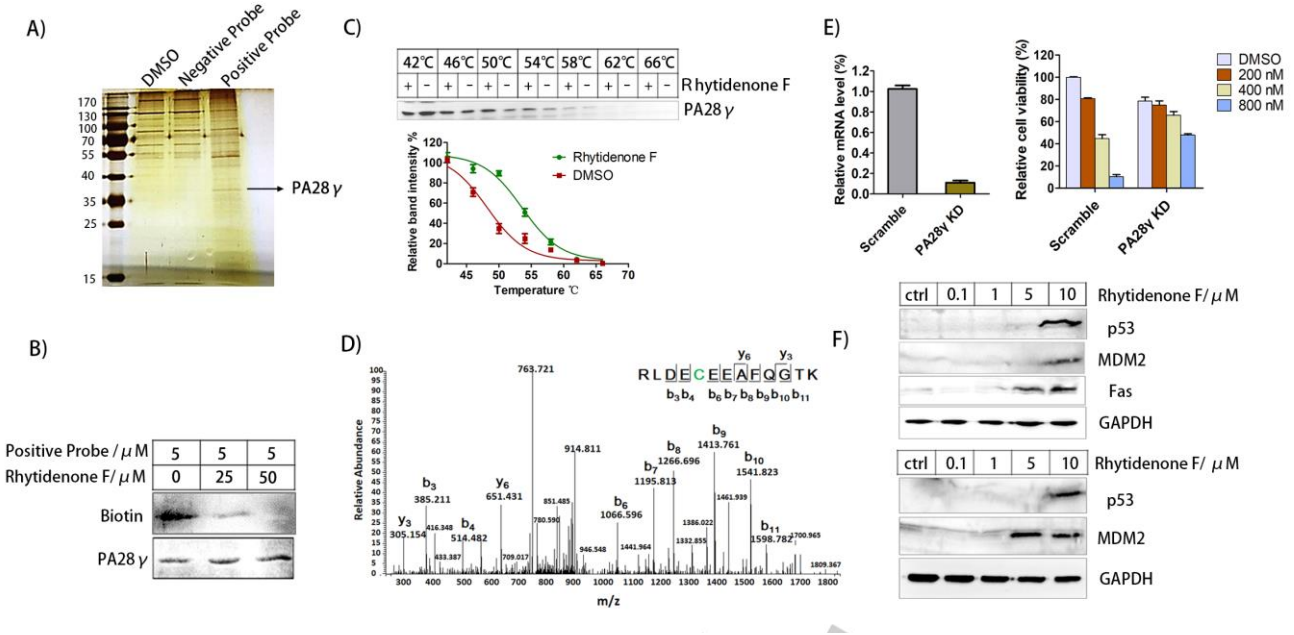

Figure 1. Rhytidenone F (**2**) directly targets PA28γ and induces p53 accumulation. A) HeLa cell lysates were incubated with negative **19** or positive probe **18** followed by pulldown with streptavidin-agarose beads and analyzed by SDS-PAGE with sliver staining. B) The recombinant PA28γ was incubated with biotin-labeled rhytidenone F in the absence or presence of unlabeled rhytidenone F for 30 min, and the mixtures were blotted for biotin or PA28γ. C) Rhytidenone F (**2**) treatment (10 μM) increased the thermal stability of PA28γ in HeLa cells as measured by the temperature-dependent cellular thermal shift assay (n = 3). D) Trypsin-digest LC-MS/MS analysis indicated modification of PA28γ with rhytidenone F (**2**) at residue cys92. E) PA28γ was knocked down in HeLa cells, and the knockdown efficiency was confirmed by qPCR (left). HeLa cells were treated with different concentration of rhytidenone F (**2**) and the cell viability was measured. HeLa cells with PA28γ knockdown were more resistant to rhytidenone F (**2**). F) HeLa cells (above) and MDA-MB-231 (below) were treated with rhytidenone F (**2**) for 24 h, followed by Western blot analysis of expression level of the indicated proteins. KD, knockdown.

have designed and synthesized the biotin-tagged positive probe **18** and the negative probe **19** for affinity purification (Scheme 3). The biological activity of the positive probe **18** is comparable to rhytidenone F (**2**), whereas the negative probe **19** is not active (Scheme 3). These two probes were used for the target identification studies.

We have performed pulldown assay using both probes **18** and **19** for the identification of the cellular target proteins of rhytidenone F (**2**). HeLa cell lysates were incubated with 10 μM negative probe **19** or positive probe **18**, followed by precipitation with streptavidin agarose beads. Proteins captured by the beads were observed on SDS-PAGE with silver staining. A band of about 30~40 kD appeared only in the cell lysates incubated with positive probe **18** (Figure 1A). Based on LC-MS/MS analysis, we have identified PA28γ as a possible candidate binding protein.

To determine if rhytidenone F (**2**) directly binds to PA28γ, we treated HeLa cells with 10 μM of this compound and detected its effect on the thermal stability of PA28γ. The cellular thermal shift assay[28] demonstrated that rhytidenone F (**2**) enhanced the stability of PA28γ at higher temperature (Figure 1C), which implied a stable interaction between rhytidenone F (**2**) and PA28γ. In addition, biotin-labeled rhytidenone F **18** also bound to the *in vitro* recombinant PA28γ protein, and this binding was competitively inhibited by higher concentrations of the unlabeled rhytidenone F (Figure 1B). To reveal the binding sites, the recombinant PA28γ was incubated with rhytidenone F (**2**), followed by LC-MS/MS analysis. The results showed a mass shift (320 Da) on the peptide RLDECEEAFQGTK, which is consistent with the addition of one molecule of rhytidenone F (**2**). Tandem mass spectrometry results revealed that Cys92 was the binding site for the covalent interaction of PA28γ and rhytidenone F (**2**) (Figure 1D).

Our next goal is to validate if PA28γ is an on-target or off-target of rhytidenone F (**2**). The bioinformatics analysis showed that PA28γ expression level has a negative correlation to some extent with the sensitivity of different cancer cell lines to rhytidenone F (**2**). K562, SK-MEL-28, MCF-7 with relatively lower PA28γ level are more resistant to rhytidenone F (Figure S2.). Furthermore, we have used lentivirus to stably knock down PA28γ gene in HeLa cells and measured the sensitivity of cells towards rhytidenone F (**2**). Comparing with the scrambled control cells, HeLa cells with PA28γ knockdown also appeared resistance to rhytidenone F (**2**) when treated with 0.2 – 0.8 μM rhytidenone F (**2**) (Figure 1E). Therefore, PA28γ is confirmed as a functional target of rhytidenone F (**2**).

10.1002/anie.201914257

PA28γ, also known as REGγ, Ki antigen or PSME3, belongs to a family of activators of the 20S proteasome that promotes the degradation of protein substrates in an ubiquitin-ATP-independent manner.[29-30] Unlike its family members PA28α and PA28β that preferentially form a heteroheptamer in the cytosol, PA28γ usually forms a homoheptamer in nucleus.[31] PA28γ is involved in the regulation of apoptosis and cell cycle progression, and PA28γ$^{-/-}$ mice displays smaller body size and increases of G_1 cells.[32] To date, the identified substrates degraded through PA28γ-dependent proteasome pathway includes steroid receptor coactivator 3 (SRC3),[33] the cell cycle regulators p21, p16, p19,[34] and hepatitis C virus core protein.[35] Notably, PA28γ promotes p53 degradation by acting as an essential cofactor that directly binds to p53 through its amino acids residues 86-96 (KRRLDECEEAF) and enhances MDM2-p53 interaction.[36] Through MDM2-p53 interaction, p53 would be polyubiquitinated and downregulated through MDM2-mediated proteasomal degradation.

Because the covalent interaction of rhytidenone F (**2**) at the Cys92 residue of PA28γ, which is located in the PA28γ-p53 binding pocket, we hypothesize the interactions of rhytidenone F and PA28γ would lead to the interference of PA28γ-p53 interactions. The MDM2-p53 interaction would subsequently be hindered and less p53 would be degraded. Accumulation of p53 can lead to cell-cycle arrest or apoptosis of cancer cells.[37-39]

We then tested this hypothesis by exposing HeLa cells to increasing concentrations of rhytidenone F (**2**) for 24 h, and evaluated the expression level of p53. As shown in Figure 2C, p53 accumulation was observed in the rhytidenone F (**2**) treated cells (HeLa cells, MDA-MB-231 cells). In addition, MDM2 was up-regulated after the rhytidenone F (**2**) treatment which is expected as MDM2 is involved in the feedback loop of the regulation of the p53 level in cells.[40] Besides, Fas, a death receptor on the surface of cells, could form the death-inducing signaling complex (DISC) and lead to programmed cell death. As a downstream substrate of p53 signaling pathway, Fas gene expression was remarkably increased accompanied by p53 accumulation. (Figure 1F)

A model of mechanism of action is proposed as described in Figure 2: To maintain a steady-state level in cells, p53 is downregulated dynamically by MDM2-mediated proteasomal degradation. In this process, PA28γ serves as a cofactor that enhances MDM2-p53 interaction and promotes p53 degradation. The covalent interaction of rhytidenone F at the Cys92 of PA28γ (a residue in PA28γ-p53 binding pocket), inhibits PA28γ-p53 interactions and hinders p53 degradation. Subsequently, accumulation of p53 activates Fas-dependent signaling pathway and initiates apoptosis of cancer cells. Moreover, we envisioned that more experiments are required to further demonstrate rhytidenone F (**2**) is relatively stable in the presence of high concentration of glutathione, which has been shown to be a major off-target *in vivo* for active small molecules with good Michael acceptor.[41] To our delight, we have discovered that glutathione does not significantly interrupt the interactions of rhytidenone F and PA28γ (Figure S3). Moreover, we have determined the half-life of rhytidenone F in pseudo-first order GSH assay is 97 minutes (Figure S4). As a comparison, the half-life of afatinib that is an FDA-approved covalent drug molecule in this assay is 25 minutes. In addition, we have purified the rhytidenone F – glutathione adducts and they also showed comparable cytotoxicity to rhytidenone F in the same assay (Table S1), suggesting a retro-Michael reaction in cells may happen to regenerate rhytidenone F and therefore give rise to the anti-tumor activity.

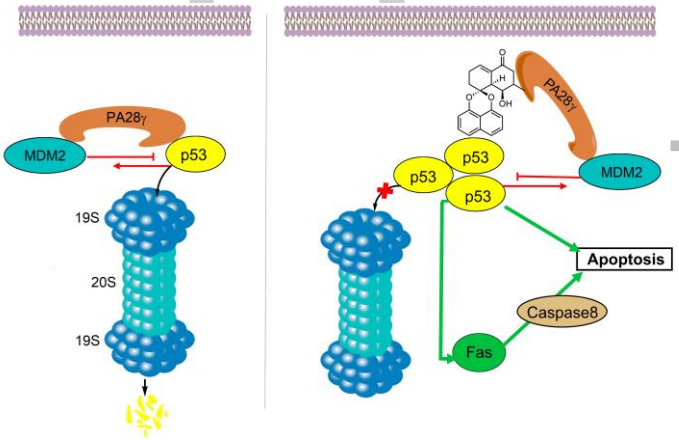

Figure 2. Proposed model of mode of action on rhytidenone F (**2**) inducing cell apoptosis.

Conclusion

The synthesis of rhytidenone A (**6**) from rhytidenone F (**2**) has been achieved via a biomimetic Michael reaction / aldol / lactonization cascade, forming 2 rings, 1 C-C bond, 2 C-O bonds, 3 new contiguous stereocenters in one step. We have further investigated the potent antitumor activity of rhytidenone F (**2**) against various cancer cell lines with IC_{50} values of 0.01 ~ 0.82 μM. The synthesis of biotin-labeled probes and pulldown assay has enabled the profiling of the cellular proteins that interacts with rhytidenone F (**2**). Interestingly, PA28γ, a negative regulator of p53, is one of the targets of rhytidenone F (**2**). Knockdown of PA28γ gene increased rhytidenone F (**2**)-resistance of HeLa cells, which demonstrates PA28γ is a functional-target of rhytidenone F (**2**). Furthermore, we have discovered that rhytidenone F (**2**) covalently attaches to Cys92 of PA28γ, which subsequently inhibits p53 degradation. The p53 accumulation activates Fas-dependent signaling pathway and initiates the apoptosis pathways. To our knowledge, rhytidenone F (**2**) is the first reported small molecule inhibitor of PA28γ that inhibits p53 degradation and induces cell apoptosis. This work presents a promising natural product lead for future anticancer drug discovery.

Experimental Section

The data for the X-ray crystallographic structures of **6**, **15** and **16** are available free of charge from the Cambridge Crystallographic Data Center under accession numbers CCDC: 1958996, 1961315, and 1961828 respectively.

Acknowledgements

We thank Prof. Jiang Zhou (Peking University) for helping with the HRMS analysis. We thank Dr. Jie Su (Peking University) for assistance with X-ray analyses, crystallographic data collection and refinement. We thank Mr. Botao Wu for assistance with computational studies. Financial support from the National Key Research and Development Program of China (2017YFA0505200), the National Natural Science Foundation of China Grant (21625201, 21661140001, 91853202, and 21521003), the Beijing Outstanding Young Scientist Program (BJJWZYJH01201910001001), and the Beijing Municipal Science and Technology Project grant (Z171100000417001) is gratefully acknowledged.

Keywords: Natural product, rhytidenone family, cell apoptosis, PA28γ, p53

[1] K. H. Vousden, D. P. Lane, *Nat. Rev. Mol. Cell Biol.* **2007**, *8*, 275-283.
[2] F. Kruiswijk, C. F. Labuschagne, K. H. Vousden, *Nat. Rev. Mol. Cell Biol.* **2015**, *16*, 393-405.
[3] C. J. Brown, S. Lain, C. S. Verma, A. R. Fersht, D. P. Lane, *Nat. Rev. Cancer* **2009**, *9*, 862-873.
[4] L. Zhou, J. Zhao, T. Shan, X. Cai, Y. Peng, *Mini-Rev. Med. Chem.* **2010**, *10*, 977-989.
[5] Y. S. Cai, Y. W. Guo, K. Krohn, *Nat. Prod. Rep.* **2010**, *27*, 1840-1870.
[6] D. J. Newman, G. M. Cragg, *J. Nat. Prod.* **2016**, *79*, 629-661.
[7] H. A. Weber, N. C. Baenziger, J. B. Gloer, *J. Am. Chem. Soc.* **1990**, *112*, 6718-6719.
[8] K. Krohn, A. Michel, U. Florke, H. J. Aust, S. Draeger, B. Schulz, *Liebigs. Ann. Chem.* **1994**, 1099-1108.
[9] P. Seephonkai, M. Isaka, P. Kittakoop, P. Palittapongarnpim, S. Kamchonwongpaisan, M. Tanticharoen, Y. Thebtaranonth, *Planta. Med.* **2002**, *68*, 45-48.
[10] S. Martinez-Luis, G. Della-Togna, P. D. Coley, T. A. Kursar, W. H. Gerwick, L. Cubilla-Rios, *J. Nat. Prod.* **2008**, *71*, 2011-2014.
[11] J. Y. Dong, H. C. Song, J. H. Li, Y. S. Tang, R. Sun, L. Wang, Y. P. Zhou, L. M. Wang, K. Z. Shen, C. R. Wang, K. Q. Zhang, *J. Nat. Prod.* **2008**, *71*, 952-956.
[12] C. E. Mcdonald, H. Holcomb, T. Leathers, F. Ampadunyarko, J. Frommer, *Tetrahedron Lett.* **1990**, *31*, 6283-6286.
[13] K. Pudhom, T. Teerawatananond, *J. Nat. Prod.* **2014**, *77*, 1962-1966.
[14] I. Siridechakorn, Z. W. Yue, Y. Mittraphab, X. G. Lei, K. Pudhom, *Bioorg. Med. Chem.* **2017**, *25*, 2878-2882.
[15] H. C. Ohishi, N.; Mikawa, T.; Sakaki, T.; Miyaji, S.; Sezaki, M., *Jpn. Pat. 01294686* **1989**.
[16] K. Pudhom, T. Teerawatananond, S. Chookpaiboon, *Mar. Drugs* **2014**, *12*, 1271-1280.
[17] R. J. Bloom, W. W. Westerfeld, *Biochemistry* **1966**, *5*, 3204.
[18] A. D. Webb, C. J. Muller, in *Advances in Applied Microbiology, Vol. 15* (Ed.: D. Perlman), Academic Press, **1972**, pp. 75-146.
[19] M. Beigi, S. Waltzer, A. Fries, L. Eggeling, G. A. Sprenger, M. Muller, *Org Lett* **2013**, *15*, 452-455.
[20] R. Noyori, S. Hashiguchi, *Acc. Chem. Res.* **1997**, *30*, 97-102.
[21] L. Z. Zhu, A. Talukdar, G. S. Zhang, J. P. Kedenburg, P. G. Wang, *Synlett* **2005**, 1547-1550.
[22] M. P. Georgiadis, S. A. Haroutounian, C. D. Apostolopoulos, *Synthesis-Stuttgart* **1991**, 379-381.
[23] B. A. Chauder, C. C. Lopes, R. S. C. Lopes, A. J. M. da Silva, V. Snieckus, *Synthesis-Stuttgart* **1998**, 279-282.
[24] B. R. Stockwell, J. P. Friedmann Angeli, H. Bayir, A. I. Bush, M. Conrad, S. J. Dixon, S. Fulda, S. Gascon, S. K. Hatzios, V. E. Kagan, K. Noel, X. Jiang, A. Linkermann, M. E. Murphy, M. Overholtzer, A. Oyagi, G. C. Pagnussat, J. Park, Q. Ran, C. S. Rosenfeld, K. Salnikow, D. Tang, F. M. Torti, S. V. Torti, S. Toyokuni, K. A. Woerpel, D. D. Zhang, *Cell* **2017**, *171*, 273-285.
[25] D. R. Green, F. Llambi, *Cold Spring Harb Perspect Biol* **2015**, *7*.
[26] S. Elmore, *Toxicol. Pathol.* **2007**, *35*, 495-516.
[27] M. Gersch, J. Kreuzer, S. A. Sieber, *Nat. Prod. Rep.* **2012**, *29*, 659-682.
[28] D. Martinez Molina, R. Jafari, M. Ignatushchenko, T. Seki, E. A. Larsson, C. Dan, L. Sreekumar, Y. Cao, P. Nordlund, *Science* **2013**, *341*, 84-87.
[29] M. Rechsteiner, C. P. Hill, *Trends Cell Biol.* **2005**, *15*, 27-33.
[30] T. Nikaido, K. Shimada, M. Shibata, M. Hata, M. Sakamoto, Y. Takasaki, C. Sato, T. Takahashi, Y. Nishida, *Clin. Exp. Immunol.* **1990**, *79*, 209-214.
[31] I. Mao, J. Liu, X. Li, H. Luo, *Cell. Mol. Life Sci.* **2008**, *65*, 3971-3980.
[32] S. Murata, H. Kawahara, S. Tohma, K. Yamamoto, M. Kasahara, Y. Nabeshima, K. Tanaka, T. Chiba, *J. Biol. Chem.* **1999**, *274*, 38211-38215.
[33] X. Li, D. M. Lonard, S. Y. Jung, A. Malovannaya, Q. Feng, J. Qin, S. Y. Tsai, M. J. Tsai, B. W. O'Malley, *Cell* **2006**, *124*, 381-392.
[34] X. Chen, L. F. Barton, Y. Chi, B. E. Clurman, J. M. Roberts, *Mol. Cell* **2007**, *26*, 843-852.
[35] K. Moriishi, T. Okabayashi, K. Nakai, K. Moriya, K. Koike, S. Murata, T. Chiba, K. Tanaka, R. Suzuki, T. Suzuki, T. Miyamura, Y. Matsuura, *J. Virol.* **2003**, *77*, 10237-10249.
[36] Z. Zhang, R. W. Zhang, *Embo. J.* **2008**, *27*, 852-864.
[37] B. Vogelstein, D. Lane, A. J. Levine, *Nature* **2000**, *408*, 307-310.
[38] X. Chen, L. J. Ko, L. Jayaraman, C. Prives, *Genes Dev.* **1996**, *10*, 2438-2451.
[39] L. T. Vassilev, B. T. Vu, B. Graves, D. Carvajal, F. Podlaski, Z. Filipovic, N. Kong, U. Kammlott, C. Lukacs, C. Klein, N. Fotouhi, E. A. Liu, *Science* **2004**, *303*, 844-848.
[40] C. L. Brooks, W. Gu, *Mol. Cell* **2006**, *21*, 307-315.
[41] R. J. Krause, R. A. Kemper, A. A. Elfarra, *Chem Res Toxicol* **2001**, *14*, 1590-1595.

10.1002/anie.201914257

WILEY-VCH

RESEARCH ARTICLE

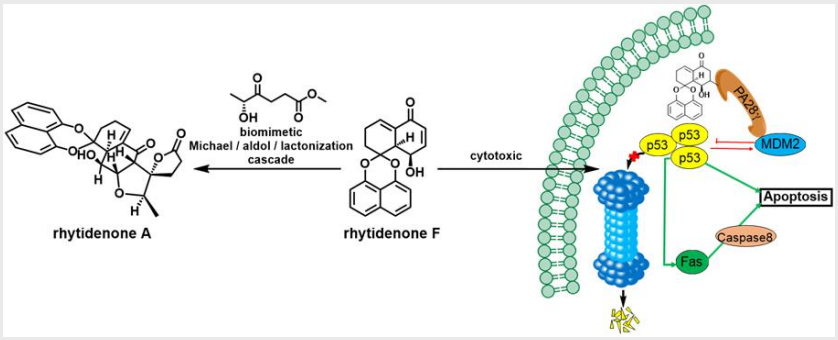

*Zongwei Yue,[+] Hiu C. Lam,[+] Kaiqi Chen, Ittipon Siridechakorn, Yaxi Liu, Khanitha Pudhom, Xiaoguang Lei**

Page No. – Page No.

Biomimetic synthesis of rhytidenone A and elucidation of mode of action of the cytotoxic rhytidenone F